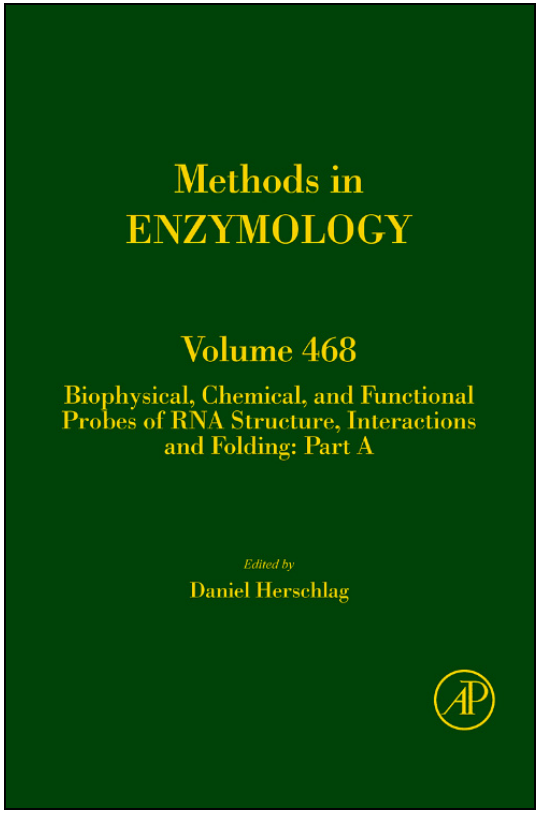

From: Marcello Forconi and Daniel Herschlag,
Use of Phosphorothioates to Identify Sites of Metal-Ion Binding in RNA
In Daniel Herschlag: Methods in Enzymology, Vol. 468,
Burlington: Academic Press, 2009, pp.311-333.
ISBN: 978-0-12-374399-2,

CHAPTER FIFTEEN

Use of Phosphorothioates to Identify Sites of Metal-Ion Binding in RNA

Marcello Forconi* *and* Daniel Herschlag†

Contents

Abstract

Single atom substitutions provide an exceptional opportunity to investigate RNA structure and function. Replacing a phosphoryl oxygen with a sulfur represents one of the most common and powerful single atom substitutions and can be used to determine the sites of metal-ion binding. Using functional assays of ribozyme catalysis, based on pre-steady-state kinetics, it is possible to extend this analysis to the transition state, capturing ligands for catalytic metal ions in this fleeting state. In conjunction with data determined from X-ray crystallography, this technique can provide a picture of the environment surrounding catalytic metal ions in both the ground state and the transition state at atomic resolution. Here, we describe the principles of such analysis, explain limitations of the method, and provide a practical example based on our results with the *Tetrahymena* group I ribozyme.

* Department of Biochemistry, Stanford University, Stanford, California, USA
† Departments of Biochemistry and Chemistry, Stanford University, Stanford, California, USA

Methods in Enzymology, Volume 468
ISSN 0076-6879, DOI: 10.1016/S0076-6879(09)68015-0

1. Introduction

The ability of RNA to express its biological function depends on the presence of divalent metal ions. Most of the divalent metal ions associated with RNA are loosely bound, in what is commonly referred to as the "ion atmosphere." These ions provide most of the positive charge needed to neutralize the enormous negative charge present on RNA. A small number of metal ions localize to particular regions of the RNA molecule and typically stabilize particular motifs and long-range contacts. For RNA enzymes, or ribozymes, metal ions may participate to the chemical transformation either directly or indirectly (see Chapter 5 of this volume).

Understanding how metal ions contribute to ribozyme function requires the identification of specific interactions made between metal ions and the RNA molecule and the assessment of the importance and role of these contacts for RNA function. X-ray crystallography provides a powerful technique to identify interactions, allowing the detection of multiple metal ions and their interactions in a single picture. Nevertheless, this picture often changes when conditions are changed, and it is not possible to establish the functionally relevant structure or the functional importance of a particular contact on the basis of structural data alone.

To address these key points functional data are needed. The use of single phosphorothioate-containing ribozymes, in conjunction with kinetic assays that assess the reactivity of these ribozymes in the presence of metal ions with high affinity for sulfur, provides a powerful means to address these key points, complementing and expanding the information obtained from structural methods. These approaches, widely applied to RNA enzymes (e.g., see Christian, 2005), were originated for studies of protein enzymes by Cohn *et al.* (1982) and Eckstein (1983).

2. Use of Phosphorothioate-Containing Ribozymes to Identify Sites of Metal-Ion Binding

2.1. Assays based on phosphorothioate substitutions on the ribozyme

Mg^{2+} is the most common cation found in RNA structures and is often found to contact an oxygen atom, typically the 2′-OH group or the negatively charged nonbridging oxygen atoms of RNA phosphoryl groups. This is not surprising, as studies with model compounds have shown that Mg^{2+} strongly prefers oxygen ligands over other type of ligands. It has been

estimated that Mg^{2+} prefers oxygen over sulfur by a factor of ~31,000-fold (Pecoraro *et al.*, 1984). This behavior is recapitulated by the hard and soft acids and bases (HSAB) theory developed by Pearson (Parr and Pearson, 1983; Pearson, 1963), stating that small, nonpolarizable (''hard'') Lewis acids strongly interact with small, nonpolarizable Lewis bases, while large, highly polarizable (''soft'') Lewis acids interact more strongly with large, highly polarizable Lewis bases. Mg^{2+} is an example of a hard Lewis acid, and oxygen ligands are hard Lewis bases; conversely, nitrogen- and sulfur-containing ligands are softer Lewis bases than those containing oxygen and interact preferentially with soft metal ions.

Because of this marked preference, a logical strategy to test putative contacts between a specific phosphoryl oxygen atom and a Mg^{2+} ion is to substitute the oxygen ligand with sulfur, introducing a thiophosphoryl group on the RNA backbone. This substitution may prevent Mg^{2+} binding, and in this case the simplest expectation is that the phosphorothioate-containing ribozyme would be significantly less reactive than the unmodified ribozyme. This situation is shown in Fig. 15.1A, where the empty circle represents the lack of a metal ion in the ground state and in the transition state of a hypothetical reaction. However, a decrease in reactivity of the modified ribozyme can arise from factors other than perturbed metal-ion binding. For example, the modified ribozyme may be defective in reactivity because of steric clashes introduced by the sulfur atom, as sulfur is larger than the native oxygen (Shannon, 1976), or because of the different hydrogen-bond properties of oxygen and sulfur (Pecoraro *et al.*, 1984; Platts *et al.*, 1996; Zhou *et al.*, 2009). In other words, there are many ways to compromise activity.

To test for effects not specific to the metal ion–sulfur contact, the reactivity of the phosphorothioate-containing ribozyme is followed as a function of a metal ion for which the preference for oxygen is not as marked as it is for Mg^{2+} or a metal ion that prefer sulfur ligands over oxygen ligands. Mn^{2+} and Cd^{2+} are two metal ions representative of these classes, respectively (Pecoraro *et al.*, 1984). Usually, these metal ions are referred to as ''more thiophilic'' (or ''softer'') than Mg^{2+}. Other metal ions used in metal ion rescue experiments include Co^{2+} and Zn^{2+}. If the functional effect is due to the lack of metal ion, because of the poor affinity of Mg^{2+} for sulfur, more thiophilic metal ions can rescue the reactivity; this rescue depends on the metal ion being able to bind in place of Mg^{2+} to the modified site. This expectation is often fulfilled in ribozymes. In the following paragraphs, we will use Cd^{2+} to describe the metal ion rescue experiments for simplicity and because this cation has been widely used (along with Mn^{2+}) in such experiments.

The simple scenario of Fig. 15.1A does not take into account the complexity of an RNA molecule. RNA-bound metal ions often have more than one inner-sphere ligands, and substituting one phosphoryl oxygen with sulfur may not be enough to remove Mg^{2+} from its binding site.

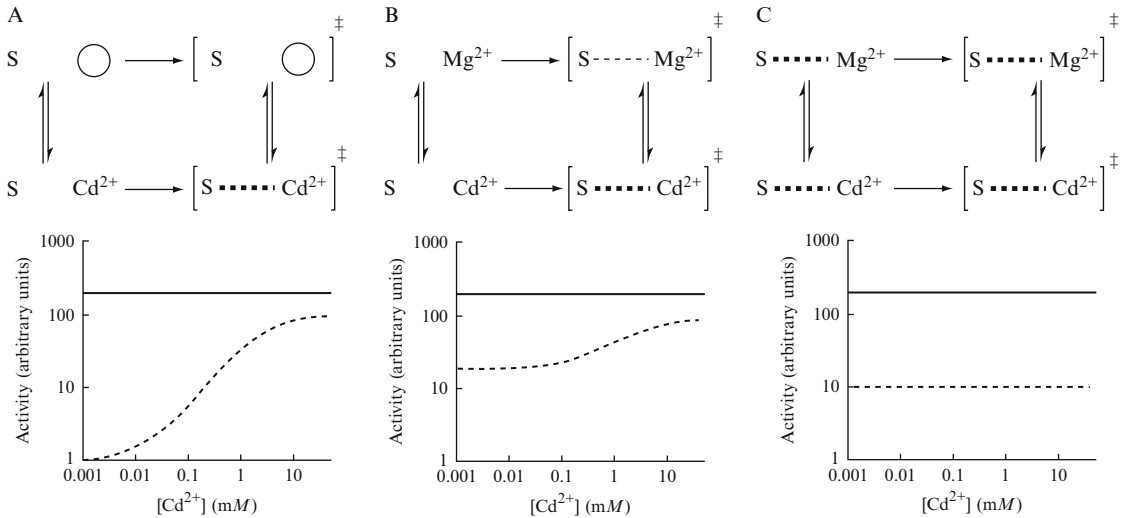

Figure 15.1 Possible situations upon the introduction of a thiophosphoryl group in the Mg^{2+}-binding site of a catalytic RNA. Upper panels: schematic representation of the interaction between the metal ion (if present) and the sulfur atom of the thiophosphoryl group in the ground state and the transition state of the reaction. Lower panels: predicted activity (arbitrary units) as a function of Cd^{2+} for the ribozyme containing the thiophosphoryl group (dashed line); the activity of the unmodified ribozyme is shown for comparison as a solid line. (A) The ribozyme containing the thiophosphoryl group is not able to bind Mg^{2+} at its original site. (B) The ribozyme containing the thiophosphoryl group can bind either Mg^{2+} or Cd^{2+}, and the contact between the metal ion and the sulfur atom is formed in the transition state only; the thicker dashes represent the stronger interaction of sulfur with Cd^{2+}. (C) The ribozyme containing the thiophosphoryl group can bind either Mg^{2+} or Cd^{2+}, and the same contact between the sulfur atom and the metal ion is formed in both the ground state and the transition state.

In this case, two more scenarios are possible, as shown in Fig. 15.1B and C. In Fig. 15.1B, Mg^{2+} is not removed upon the phosphorothioate substitution, but the contact between the sulfur atom of the ligand and this metal ion becomes stronger in the transition state (compared to the ground state). This could be due to a movement of the ligand as the reaction proceeds or, in the extreme case, to a contact that is formed only in the transition state. When Cd^{2+} occupies the metal-ion binding site, there is advantage over Mg^{2+} in the transition state, because of the stronger interaction that can be formed between Cd^{2+} and sulfur, compared to Mg^{2+} and sulfur. In this case, the activity of the modified ribozyme in Cd^{2+} is predicted to increase compared to Mg^{2+}.

In the scenario of Fig. 15.1C, the contact between the metal ion and the sulfur atom is formed in both the ground state and the transition state, regardless of the nature of the metal ion present in the binding site. In this case, there may be no advantage in having Cd^{2+} over Mg^{2+} in the metal-ion binding site, and the activity of the modified ribozyme is predicted, in the simplest case, to remain the same even if Cd^{2+} binds to the Mg^{2+}-binding site. This lack of a Cd^{2+} effect on the activity is analogous to what expected if the introduced sulfur atom does not contact a metal ion or if the metal ion cannot bind anymore at its site because of the introduction of a sulfur atom. Therefore, an alternative approach has to be undertaken to distinguish between these situations and to functionally identify the site in question as of metal-ion binding. One such approach is described in Section 2.2.

Thiophilic metal ions can affect steps other than the chemical step. For example, in the *Tetrahymena* group I ribozyme, Mn^{2+} stimulates a conformational change, speeding reactions that involve this conformational change (Shan and Herschlag, 2000). Further, in some cases a nonchemical rate-limiting step, which is rescued by Cd^{2+}, has been observed for the modified but not the unmodified ribozymes (Hougland *et al.,* 2005; M.F. and D.H. unpublished results). In these cases, the observation of an increase in the activity of the modified ribozyme when Mn^{2+} or Cd^{2+} is added may not be indicative of involvement of a metal ion important for the chemical transformation, as these ribozymes may react from a ground state that is different from that of the unmodified ribozyme or have an additional nonchemical rate-limiting step. Thus, it is crucial to perform appropriate controls to test that the unmodified and modified ribozymes react from the same ground state, and detailed pre-steady-state kinetic analysis is typically required.

Population experiments, such as nucleotide analog interference mapping (NAIM), whereby pools of ribozymes containing a single phosphorothioate substitution are prepared by *in vitro* transcription and their activity assayed in "standard conditions", have been extremely powerful for initial screening of candidates for metal-ion binding (Christian and Yarus, 1993; Harris and Pace, 1995; Jansen *et al.,* 2006; Kazantsev and Pace, 1998; Luptak and

Doudna, 2004; Sood *et al.,* 1998; Strauss-Soukup and Strobel, 2000). Indeed, such information can be obtained even when crystal structures are lacking. Nevertheless, to strongly implicate a particular phosphoryl oxygen in metal-ion binding, the phosphorothioate-containing ribozyme must be investigated in detailed kinetics experiments that take into account the concerns about the individual reaction steps being monitored. In principle, such experiments can be carried out on populations of molecules (Hertel *et al.,* 1996), but analysis of such data would be difficult and has not been fully developed.

2.2. Coupling phosphorothioate substitution on the ribozyme with atomic substitutions on the substrate

As described above, a situation in which the phosphorothioate substitution does not disrupt binding of Mg^{2+}, shown in Fig. 15.1C, is predicted to result in no change of activity of the modified ribozyme over increasing Cd^{2+} concentration. In terms of reactivity, this situation would be equivalent to a situation in which the sulfur atom introduces steric clashes, but does not contact a metal ion and thus the reactivity of the modified ribozyme cannot be rescued by Cd^{2+} addition, or a situation in which Cd^{2+} cannot substitute for Mg^{2+} at the metal-ion binding site. To distinguish among these possibilities, one needs a way to measure the affinity of the rescuing Cd^{2+} and compare with the unmodified ribozyme. If the sulfur atom of the introduced thiophosphoryl group contacts the rescuing Cd^{2+}, this affinity is expected to be higher for the phosphorothioate-containing ribozyme (compared to the unmodified ribozyme) because of the favorable Cd^{2+}–sulfur contact. Conversely, if the sulfur atom introduced on the ribozyme is deleterious for reasons other than metal-ion coordination, the affinity of the rescuing Cd^{2+} is predicted to be the same of that of the unmodified ribozyme, because no change in ligand coordination is expected between the modified and unmodified ribozymes. Nevertheless, more complex scenarios are also possible that include, for example, alterations in binding site geometry.

One way to measure the affinity for such ''hidden'' metal ions, and to obtain additional atomic-level information, involves coupling phosphorothioate substitution on the ribozyme with an analogous substitution on the substrate. An example is given below with the *Tetrahymena* group I ribozyme.

2.2.1. Thermodynamic Fingerprint Analysis (TFA) using the *Tetrahymena* group I ribozyme

The *Tetrahymena* group I ribozyme catalyzes a nucleotidyl transfer reaction from an oligonucleotide substrate (S), which mimics the natural 5′-splice site, to an exogenous guanosine (G), which serves as the nucleophile; the

reaction is analogous to the first step of group I intron self-splicing (Eq. (15.1); Herschlag and Cech, 1990; Zaug *et al.*, 1988).

$$\underset{(S)}{CCCUCUA} + G_{OH} \rightarrow \underset{(P)}{CCCUCU_{OH}} + GA \qquad (15.1)$$

Early metal-ion rescue experiments identified four transition state contacts between metal ions and atoms on the substrates through use of thio- and amino-substituted substrates and provided evidence against metal ion interactions at other positions (Liao *et al.*, 2001; Piccirilli *et al.*, 1993; Rajagopal *et al.*, 1989; Shan and Herschlag, 1999; Sjogren *et al.*, 1997; Weinstein *et al.*, 1997; Yoshida *et al.*, 1999, 2000). The substrate atoms involved in metal ion coordination are shown in Fig. 15.2.

The number of metal ions making contacts with these atoms can be determined by a quantitative approach called "Thermodynamic Fingerprint Analysis" (Shan and Herschlag, 1999; Shan *et al.*, 2001; Wang *et al.*, 1999), or TFA, which is described below.

Consider two substrates, S_o and S_x, corresponding to an unmodified and sulfur- or nitrogen-modified substrate. For example, S_x can represent an oligonucleotide substrate with a 3′-bridging sulfur on the leaving group (Piccirilli *et al.*, 1993). Schemes 15.1A and B show generic reaction frameworks for the unmodified (or cognate) and modified substrates, respectively. In Schemes 15.1A and B, the reaction rate reflects the fraction of ribozyme

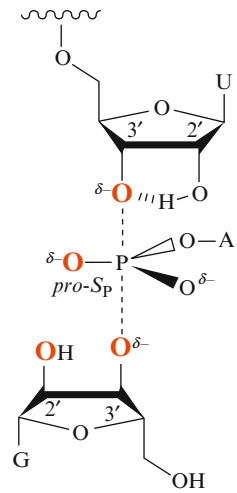

Figure 15.2 Schematic representation of the transition state for the reaction of the *Tetrahymena* group I ribozyme. Oxygen atoms indicated in bold have been linked to metal ion coordination by sulfur substitution or, for the 2′-OH of guanosine, by amino group substitution.

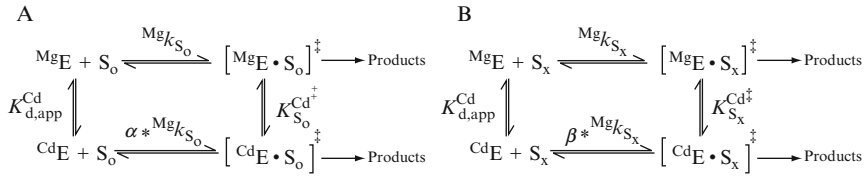

Scheme 15.1 General reaction frameworks for the unmodified (S_O, panel A) and modified (S_X, panel B) substrates with and without bound Cd^{2+}, in a background of Mg^{2+} . Charges on metal ions are omitted for clarity.

that has Cd^{2+} bound, with a rate enhancement with saturating Cd^{2+} given by the parameters α and β for S_o and S_x, respectively. The Cd^{2+} concentration dependence of the observed rate constants gives the dissociation constant for Cd^{2+}, $K^{Cd}_{d,app}$, as shown in Eqs. (15.2a) and (15.2b). Because experiments are carried out in a background of Mg^{2+} to ensure proper folding of the ribozyme, this value is an "apparent affinity" that depends on the Mg^{2+} concentration present in solution.

$$k^{S_o}_{obs} = {}^{Mg}k_{S_o}\left[\frac{K^{Cd}_{d,app} + \alpha[Cd^{2+}]}{K^{Cd}_{d,app} + [Cd^{2+}]}\right] \tag{15.2a}$$

$$k^{S_x}_{obs} = {}^{Mg}k_{S_x}\left[\frac{K^{Cd}_{d,app} + \beta[Cd^{2+}]}{K^{Cd}_{d,app} + [Cd^{2+}]}\right] \tag{15.2b}$$

There are two critical features of this analysis. First, $K^{Cd}_{d,app}$ represents binding of Cd^{2+} to the reaction's ground state, even though it is determined by following a reaction rate that represents transient attainment of the reaction's transition state; nevertheless, $K^{Cd}_{d,app}$is linked to the transition state affinities, $K^{Cd\,\ddagger}_{S_O}$ and $K^{Cd\,\ddagger}_{S_x}$, via the thermodynamic cycle shown in Scheme 15.1, such that $K^{Cd\,\ddagger}_{S_O} = K^{Cd}_{d,app}/\alpha$ and $K^{Cd\,\ddagger}_{S_X} = K^{Cd}_{d,app}/\beta$. Second, the reaction's ground state is the free ribozyme and free substrates so that the substrate modification has no affect on the affinity of Cd^{2+} for the ribozyme. In practice, experiments are sometimes carried out with certain substrates bound, provided that control experiments have determined that the association of those substrates is not coupled to the binding of the rescuing metal ion, that is, that the binding of such substrates does not affect the dissociation constant for the rescuing metal ion (Forconi *et al.,* 2008; Hougland *et al.*, 2005, 2006; Shan *et al.,* 1999).

A complication in metal-ion rescue experiments with RNA arises from the large number of associated metal ions. Because of this, metal ions can bind at sites other than the one involved in rescue and affect activity. In many cases, high concentrations of thiophilic metal ions cause inhibition of the normal reaction, apparently by binding at one or more alternate sites.

There can also be stimulatory effects from occupancy of other sites. If these effects are the same with the normal and the modified substrate, they are readily eliminated by using a *relative* rate constant, k_{rel}, which is simply the ratio of rate constants for the modified and unmodified substrates at each Cd^{2+} concentration, as shown in Eq. (15.3). This situation often holds, and this approach has been used on multiple occasions (Forconi *et al.,* 2008; Gordon and Piccirilli, 2001; Shan and Herschlag, 1999; Shan *et al.,* 2001; Sun and Harris, 2007; Wang *et al.,* 1999). Further, experiments are usually carried out in a background of high Mg^{2+} to minimize the effects from binding of the soft metal ions at other sites. Nevertheless, the possibility of binding of thiophilic metal ions at alternate sites that give differential effects on reactions of the cognate and modified substrates often cannot be eliminated and cannot be accounted for in a straightforward manner. In such cases, rescue experiments must look for consistency among multiple probes and experiments.

$$k_{rel} = {}^{Mg}k_{rel}\left[\frac{K_{d,app}^{Cd} + \beta[Cd^{2+}]}{K_{d,app}^{Cd} + \alpha[Cd^{2+}]}\right]; \quad {}^{Mg}k_{rel} = \frac{{}^{Mg}k_{S_x}}{{}^{Mg}k_{S_o}} \tag{15.3}$$

We return to the straightforward case of an unmodified ribozyme in which Cd^{2+} does not affect the reactivity of the unmodified substrate, S_o, except for nonspecific inhibition at high Cd^{2+} concentration that can be taken into account by the use of k_{rel} (Shan *et al.,* 2001); therefore, the parameter α in Scheme 15.1 and Eq. (15.3) is equal to 1. This simplifies Eq. (15.3) to Eq. (15.4). In Eq. (15.4), ${}^{Mg}k_{rel}$ and β can be easily determined, because they represent the value of k_{rel} in the absence of Cd^{2+} and the increase of k_{rel} at saturating Cd^{2+} concentration, respectively. Further, the value of $K_{d,app}^{Cd}$ can be precisely determined by plotting k_{rel} versus Cd^{2+} concentration and fitting to Eq. (15.4)).

$$k_{rel} = {}^{Mg}k_{rel}\left[\frac{K_{d,app}^{Cd} + \beta[Cd^{2+}]}{K_{d,app}^{Cd} + [Cd^{2+}]}\right]; \quad {}^{Mg}k_{rel} = \frac{{}^{Mg}k_{S_x}}{{}^{Mg}k_{S_o}} \tag{15.4}$$

For each substrate modification, the value of $K_{d,app}^{Cd}$ provides a ''fingerprint'' for the binding to the free ribozyme of the metal ion that rescues that particular substrate modification. If the rescue profiles obtained for two different substrate modifications have different $K_{d,app}^{Cd}$, this is a strong indication that distinct metal ions rescue each modification. If the values are the same, it is possible that the same site is involved or that different sites coincidentally have similar Cd^{2+} affinities. In this case, additional experiments are carried out to determine if one or two Cd^{2+} ions are required to rescue the two substrate modifications (Shan *et al.*, 2001; Wang *et al.*, 1999). Additional evidence can be obtained by perturbing individual metal-ion binding sites, as described below.

2.2.2. Introducing phosphorothioate substitution on the ribozyme

To determine ribozyme ligands for a particular metal ion, one most simply determines whether a phosphorothioate substitution on the ribozyme results in a higher affinity of the rescuing Cd^{2+}. In graphical terms, a lower $K_{d,app}^{Cd}$ (higher affinity) will manifest itself in a shift of the rescuing profile to lower Cd^{2+} values (Fig. 15.3; compare the gray lines to the black line). This effect holds regardless of the effect of Cd^{2+} on the reaction of the unmodified substrate (S_o) with the modified ribozyme, which can be neutral (Fig. 15.1C, corresponding to $\alpha = 1$ in Scheme 15.1A and resulting in the rescue profile shown in Fig. 15.3A), inhibitory (e.g., because the contact between the Cd^{2+} ion and the sulfur atom on the ribozyme needs to be broken to attain the transition state, corresponding to $\alpha < 1$ in Scheme 15.1A and resulting in the rescue profile shown in Fig. 15.3B), or stimulatory (Fig. 15.1A and B, corresponding to $\alpha > 1$ in Scheme 15.1A and resulting in the rescue profile shown in Fig. 15.3C).

Although the shape of the curves is the same in Fig. 15.3A–C, fitting the experimental k_{rel} values to Eq. (15.4) will give a misleading value of $K_{d,app}^{Cd}$ in the situations described by Fig. 15.3B and C (i.e., when Cd^{2+} affects the reactivity of the unmodified substrate in the phosphorothioate-containing ribozyme). In the examples shown in Fig. 15.3, fitting the gray curves in Fig. 15.3A–C to Eq. (15.4) gives values of $K_{d,app}^{Cd} = 0.2$, 2, and 0.002 m*M*, respectively, although the true value of $K_{d,app}^{Cd}$ is 0.2 m*M* in all of the three cases. Put another way, the value of $K_{d,app}^{Cd}$ determined from fitting to Eq. (15.4) corresponds to the true $K_{d,app}^{Cd}$ divided by α. Thus, if Cd^{2+} affects the reactivity of the unmodified substrate, S_o, in the phosphorothioate-containing ribozyme, Eq. (15.3) must be used to determine the correct value of $K_{d,app}^{Cd}$. However, in the absence of other information that allow to determine which Cd^{2+} ion is responsible for the stimulatory (or inhibitory) effect on the reaction of the unmodified substrate, it is often not possible to determine the value of α and therefore the value of $K_{d,app}^{Cd}$. Nevertheless, the shift in the rescuing profile remains a signature for an interaction between the sulfur atom on the ribozyme and the rescuing Cd^{2+} ion (Fig. 15.3A–C).

In ideal situations, the affinity of the rescuing metal ion is affected only by direct effects. In practice, indirect effects from altered charge distributions, steric clashes, and structural rearrangements upon substitution of sulfur for oxygen can result in changes in the affinity for a rescuing metal ion. Nevertheless, direct contacts will generally induce larger changes in the metal ion affinity compared to indirect effects. Thus, it is also important to determine the magnitude of effects arising from sulfur substitutions at a variety of positions.

TFA coupled with the introduction of phosphorothioate substitutions on the ribozyme has been successfully used in the *Tetrahymena* group I ribozyme to establish ligands for the catalytic metal ions. Among the many

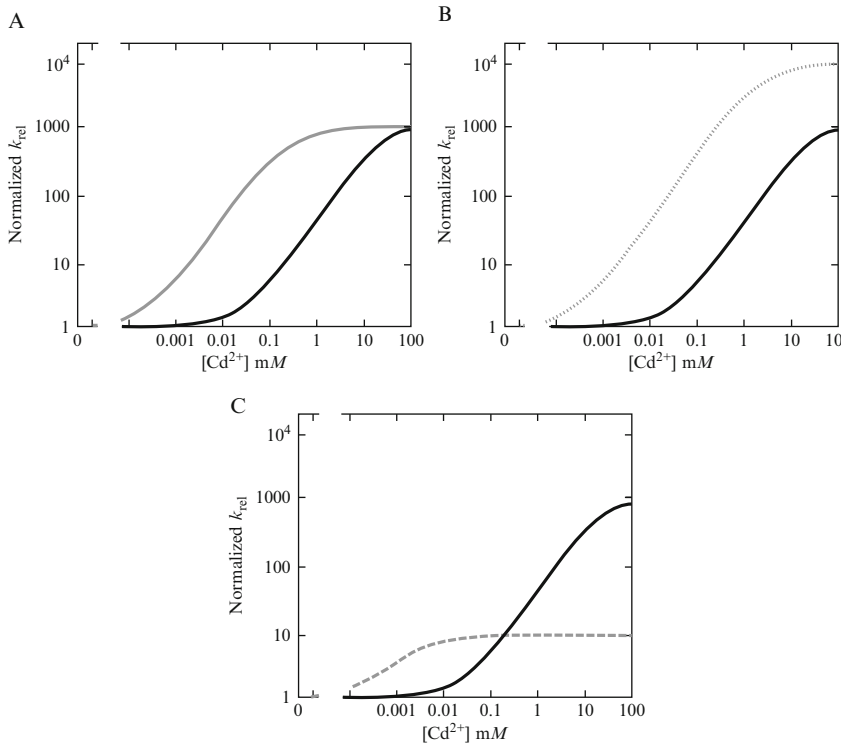

Figure 15.3 Expected trend of k_{rel} profiles (see text for details) for the unmodified ribozyme (black line) and for a ribozyme in which the introduced thiophosphoryl group makes a contact with a metal ion in both the ground state and the transition state (gray lines). k_{rel} is normalized for each ribozyme such that its value is equal to 1 in the absence of Cd^{2+}. In the simulations, β, which represents the rate enhancement of S_x with the metal-ion binding site saturated with Cd^{2+}, is set to 1000 for all ribozymes; $K_{d,app}^{Cd} = 20$ mM and 0.2 mM for the modified and unmodified ribozymes, respectively. (A) The Cd^{2+} that rescues reactivity of the modified substrate, S_x, has no effect on the reactivity of the unmodified substrate, S_o, in the modified ribozyme (solid gray line, $\alpha = 1$, Eq. (15.3)). (B) The Cd^{2+} that rescues reactivity of the modified substrate, S_x, has an inhibitory effect on the reactivity of the unmodified substrate, S_o, in the modified ribozyme (dotted gray line, $\alpha = 0.1$, Eq. (15.3)). (C) The Cd^{2+} that rescues reactivity of the modified substrate, S_x, has an inhibitory effect on the reactivity of the unmodified substrate, S_o, in the modified ribozyme (dashed gray line, $\alpha = 100$, Eq. (15.3)). The black line is the same in all the three panels, and is repeated for ease of comparison.

phosphorothioate substitutions introduced in the RNA backbone of the *Tetrahymena* ribozyme, only the ones predicted from crystal structures (Golden *et al.*, 2005; Guo *et al.*, 2005; Lipchock and Strobel, 2008; Stahley and Strobel, 2005) to contact a metal ion showed increasing Cd^{2+} ground state and transition state affinity compared to the unmodified ribozyme (Forconi *et al.*, 2007, 2008; Hougland *et al.*, 2005; M.F and

D.H., unpublished results). Analogous studies have been performed with the hammerhead (Wang *et al.*, 1999), the RNase P (Christian *et al.*, 2002), and the group II (Gordon and Piccirilli, 2001) ribozymes. In the following protocol, we describe how we have successfully introduced the phosphorothioate modification in the *Tetrahymena* ribozyme, performed kinetic tests and determined the ground state and transition state affinities for Cd^{2+}. This approach can be extended to other ribozymes, providing that:

1. The chemical step is followed in all the reactions monitored;
2. Proper controls are taken to ensure that the ground states of the unmodified and modified ribozymes are the same.

3. Protocols

3.1. Preparation of phosphorothioate-containing ribozymes

Working with RNA presents serious challenges, because of the prevalence of nucleases. Therefore, it is essential to work in "RNase-free" conditions. This involves the use of certified RNase-free plastic tubes and pipette tips, filtering water and reagents through a 0.2 μm filter, and changing gloves often.

3.1.1. General considerations on construction of phosphorothioate-containing RNA

Short (<80 nucleotides) RNAs containing a single phosphorothioate modification can be obtained by chemical synthesis.

Larger RNAs with a single phosphorothioate substitution are obtained by ligating a chemically synthesized RNA oligonucleotide (that contains the phosphorothioate modification) to the rest of the RNA molecule (Forconi *et al.*, 2007, 2008; Moore and Sharp, 1992). Depending on the position of the site of the modification and the length of the target RNA, this ligation can involve two or three pieces. Ligations with more pieces are also possible, if two or more modifications need to be introduced simultaneously. However, yields of fully ligated RNA decrease significantly with increasing number of pieces. Here, we describe a protocol for a three-piece ligation (Fig. 15.4), using transcribed RNA on the flanking regions and a chemically synthesized oligonucleotide, containing the phosphorothioate modification, in the middle piece. This protocol can be easily adapted to other situations.

Regardless of the number of pieces, RNA pieces can usually be ligated in a one-pot reaction using DNA ligase. DNA ligase joins RNA containing a 3'-hydroxyl group to RNA containing a 5′-phosphoryl group in a splint-assisted manner. Therefore, the pieces used in the ligation have to be prepared taking into account these requirements. Recent results (Ho and

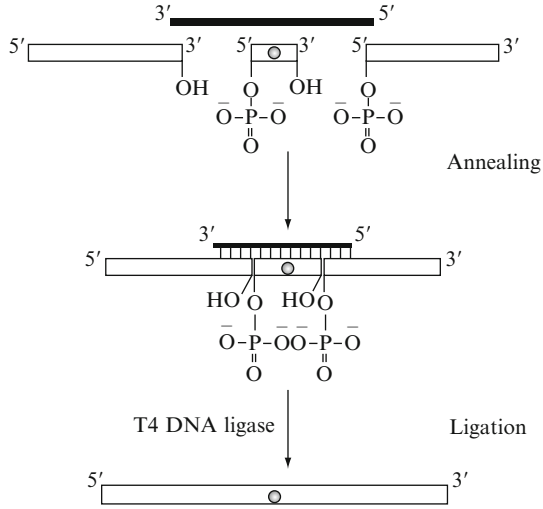

Figure 15.4 Schematic representation of the protocol for ligation of a fragment containing the phosphorothioate modification (represented by a gray sphere).

Shuman, 2002) suggest that RNA ligase 2, which also ligates RNA in a splint-assisted manner, can be used instead of DNA ligase, but we have not evaluated the efficiency and fidelity of this enzyme.

Ideally, the piece containing the phosphorothioate should be long enough to be specifically annealed to the splint, but shorter than 20 nucleotides so that the two phosphorothioate diastereoisomers can be easily separated by HPLC (see Section 3.1.6 and Chapter 14 of this volume). Diastereoisomers of oligonucleotides containing a phosphorothioate near the 5′-end are generally easier to separate by HPLC than diastereoisomers of oligonucleotides with a phosphorothioate near the 3′-end.

3.1.2. Transcription of the 5′-piece

Always run a test transcription to optimize reaction conditions for each construct, varying concentration of DNA template, quantity of RNA polymerase, and time of reaction. Once conditions are optimized, run a large-scale transcription. The values below are used for transcription of the region corresponding to nucleotides 22–296 of the *Tetrahymena* ribozyme and represent guidelines for other constructs. To ensure homogeneity of the 3′-ends, the transcript should have a 3′-hammerhead or HDV ribozyme (contained in the DNA template), that will self-cleave in transcription conditions; other cleavage strategies are also possible (Morl *et al.*, 2005). These cleavage elements leave an RNA with a terminal 2′,3′-cyclic phosphate; removal of this group is described in Section 3.1.5.

	Final concentration	Test transcription	Large-scale transcription
10× transcription buffer (400 m*M* Tris–HCl, pH 7.9; 60 m*M* $MgCl_2$; 100 m*M* NaCl; 20 m*M* spermidine)	1×	10 μl	1.0 ml
1 *M* dithiothreitol	40 m*M*	4 μl	0.4 ml
Mixture of NTPs, 10 m*M* each	2 m*M*	20 μl	2.0 ml
DNA template, ~20 μg/ml	1 μg/ml	5 μl	0.5 ml
T7 RNA polymerase, 20,000 units/ml	200 units/ml	1 μl	0.1 ml
H_2O		60 μl	6.0 ml
Total		100 μl	10.0 ml

(a) Combine reaction components, adding the DNA at last.
(b) Incubate at 37 °C for at least 3 h. For a quick test to determine whether RNA is being transcribed or not, run an aliquot of the reaction on a 2% denaturing agarose gel.
(c) To quench the reaction, add 250 m*M* EDTA, pH 8.2, to a final concentration of 50 m*M*.
(d) Precipitate the RNA by adding 0.5 volumes of 7.5 *M* ammonium acetate and 3 volumes of cold ethanol. Incubate for at least 30 min at −20 °C. Longer incubation times (overnight) can also be used.
(e) Spin the solution at 14,000 rpm for 15–30 min.
(f) Remove the supernatant and store it. Dissolve the pellet in an appropriate volume of loading buffer (10 m*M* EDTA, 90% formamide, 0.01% bromophenol blue, 0.01% xylene cyanol) and purify the RNA by gel electrophoresis, as described in Section 3.1.4.

3.1.3. Transcription of the 3′-piece

For splint ligations, the 3′-piece needs to be 5′-phosphorylated. This form can be achieved by adding at least a fivefold excess of 5′-GMP over GMP to the reaction in Eq. (15.1). The reaction protocol is otherwise the same.

In this particular case, homogeneity of the 3′-end of this piece is usually not critical; otherwise, methods analogous to those described for the homogeneity of the 5′-piece (see Section 3.1.2) can be used.

3.1.4. Gel purification of transcripts

Prepare the polyacrylamide gel in 7.5 *M* urea/1× TBE (90 m*M* Tris–borate, pH 8.5, 2.5 m*M* EDTA). Adjust the percentage of acrylamide depending on the size of the RNA to be purified. The thickness of the gel should be adjusted according to the amount of RNA to be loaded. For the particular 10 ml transcription mentioned in Section 3.1.2, we use 8% acrylamide, 3 mm thick gels, and load the RNA on one or two gels containing two 35-mm-long wells. Yields from a 10 ml transcription are typically 20–50 nmol after gel purification.

(a) Pre-run the gel using 1× TBE buffer for at least 30 min (65 W for a 3 mm thick gel). Use a metal plate to distribute heat evenly on the glass plate and prevent it from cracking.
(b) Load the sample (with the gel off) and run the gel at 65 W for the appropriate amount of time. Use charts (Maniatis *et al.*, 1975) to determine where the RNA runs compared to the dyes present in the loading buffer.
(c) Separate the plates and place the gel between saran wrap (both sides).
(d) Visualize the RNA bands using UV shadowing. Use a pen to indicate the location of the bands. Avoid damage of RNA by the UV light by minimizing its exposure.
(e) Cut out the bands using a sterilized razor blade or scalpel. It is possible that some of the hammerhead-containing construct is still present on the gel. This species migrates slower than the cleaved RNA. In this case, cut both bands and analyze them afterwards on denaturing PAGE. Place the gel slices in a conical tube. Use ethanol-washed, RNase-free glass rods to crush the RNA. Use a different glass rod for each different RNA.
(f) Add 1–2 volumes of elution buffer (50 m*M* Tris–HCl, pH 7.5; 10 m*M* EDTA; 0.3 *M* NaCl) to the excised bands. Elute the RNA overnight at 4 °C using a tube rotator.
(g) Spin down the samples using a swinging bucket centrifuge (5000×*g*). Immediately separate the supernatant from the gel pieces by using a syringe and a 0.2 or 0.45 μm filter. To increase the yields, repeat the extraction by adding more elution buffer to the gel pieces and eluting overnight as in step (f).
(h) Ethanol precipitate the RNA by adding 0.5 volumes of 3 *M* NaCl and 2.5 volumes of ice-cold ethanol. Incubate at −20 °C for at least 30 min.
(i) Spin the solution at 14,000 rpm for 15–30 min.
(j) Wash the pellet with 70% ethanol and dissolve it in water or buffer.

(k) Determine the concentration of the transcripts by UV spectrophotometry. Check the length and homogeneity of the construct by denaturing PAGE, alongside standards of known length.

3.1.5. Removal of 2′,3′-cyclic phosphate from the 5′-piece

Several methods are available for this operation (Morl *et al.*, 2005). Here, we describe a method that has worked with our constructs. The reaction can be scaled down depending on the quantity of RNA. To scale up, we typically run multiple reactions.

Set up the following reaction:

	Final concentration	**Volume (μl)**
1 *M* imidazole–HCl, pH 6	100 m*M*	63
1 *M* $MgCl_2$	10 m*M*	6.3
RNA, ~50 μ*M*	16 μ*M*	200
10 m*M* 2-mercaptoethanol	70 μ*M*	4.4
100 μg/ml BSA (RNase free)	19 μg/ml	120
T4 polynucleotide kinase, (10,000 units/ml)	200 units/ml	13.0
H_2O		223
Total		630

(a) Incubate at 37 °C for 6 h.
(b) Check the pH of the solution. If it is too low (<6), raise it to 7–8 by using an appropriate buffer; otherwise, the RNA will not be extracted correctly in the following step.
(c) Split the solution in an appropriate number of tubes and add 1 volume of phenol/chloroform/isoamyl alcohol solution (25:24:1, pH 8.0).
(d) Vortex and spin the samples. Separate the aqueous and organic layers.
(e) Mix each aqueous layer with 1 volume of chloroform.
(f) Vortex and spin the samples. Separate the aqueous layers.
(g) Pool together the aqueous layers of the same RNA.
(h) Back extract the phenol/chloroform/isoamyl alcohol solution with water or 10 m*M* Tris, pH 7.5. Vortex and spin the samples. Use this aqueous layer to back extract the RNA from the chloroform layer. Pool together the aqueous layers of the same RNA from the back extractions.
(i) Add 0.5 volumes of NaCl and 2.5 volumes of cold ethanol to each aqueous layer. Precipitate the RNA at −20 °C overnight.
(j) Spin the samples for 15 min at 15,000 rpm.
(k) Redissolve the RNA pellet in water and determine the concentration of RNA by UV spectrophotometry.

3.1.6. HPLC purification of phosphorothioate-containing oligonucleotides

Oligonucleotides should contain a 5′-phosphoryl group. The phosphorothioate diastereoisomers are purified using ion-exchange HPLC. Typical buffers used are:

Buffer A: 20 m*M* Tris, pH 7.6

Buffer B: 20 m*M* Tris, pH 7.6; 1 *M* NaCl

Elution times vary with the RNA construct. For a 15-mer with a phosphorothioate near the 5′-end, a gradient of 37–50% of B over 30 min affords good separation of the diastereoisomers.

Diastereoisomers of oligonucleotides containing a phosphorothioate near the 3′-end may not be separable using this technique. In this case, we have successfully separated the isomers by annealing to a oligodeoxyribonucleotide of complementary sequence (Forconi *et al.*, 2007). Separation of the DNA and RNA oligonucleotides was achieved by reverse-phase HPLC under denaturing conditions (Forconi *et al.*, 2007).

3.1.7. Ligation reaction

Ligation reactions are carried out in two parts. First, the RNA pieces are annealed on the DNA splint. This is achieved by heating the RNA to 90 °C, disrupting base pairs within the RNA, and slowly cooling down to room temperature. Second, the annealed solutions are mixed with the enzyme and left to react.

Always prepare a variant without the phosphorothioate modification (unmodified ribozyme) and compare its kinetic properties to those of the transcribed ribozyme. These properties should be identical.

3.1.7.1. Annealing step

	Final concentration	**Test ligation (μl)**	**Large-scale ligation (μl)**
3′-piece, 100 μ*M*	10 μ*M*	2.5	60
Middle piece (with phosphorothioate), 100 μ*M*	10 μ*M*	2.5	60
5′-piece, 100 μ*M*	10 μ*M*	2.5	60
DNA splint, 100 μ*M*	10 μ*M*	2.5	60
0.5 *M* NaCl	100 m*M*	5.0	–
3 *M* NaCl	100 m*M*	–	20
100 m*M* Tris, pH 7.5; 10 m*M* EDTA	10 m*M* Tris, 1 m*M* EDTA	2.5	60
H_2O		7.5	280
Total		25	600

(a) Prepare the above solution in a single Eppendorf tube. Gently vortex and spin.
(b) Heat the solution at 90 °C for 1 min.
(c) Allow the solution to cool slowly to room temperature.
(d) Steps (b) and (c) can be performed using a PCR machine. In this case, split large ligations in several tubes (maximum 100 μl of solution in each tube) to allow proper annealing.

3.1.7.2. Ligation

	Test ligation (μl)	**Large ligation (μl)**
10× ligase buffer (660 m*M* Tris–HCl, pH 7.6; 80 m*M* $MgCl_2$; 100 m*M* DTT; 1 m*M* ATP; 0.04% Triton X-100)	2.0	600
Annealed solution from previous step	2.0	600
RNasin 0.2 units/μl	2.0	–
RNasin 20 units/μl	–	6.0
T4 DNA ligase, 10 μ*M*	4.0	–
T4 DNA ligase, 100 μ*M*	–	120
H_2O	10	4670
Total	20	6000

(a) Prepare the reaction solution. Mix by pipetting up and down.
(b) Incubate at room temperature overnight (12–18 h). Longer or shorter times can be used; for longer times, fresh RNasin added to the solution after overnight incubation is sometimes helpful. However, RNA degradation may become an issue after 20 h.
(c) Precipitate the RNA and purify it on polyacrylamide denaturating gel as described for transcription reactions in Section 3.1.2.

Always consider the following:

- The concentration of T4 DNA ligase should be equal to the RNA concentration multiplied by the number of junctions. However, different preparations of T4 DNA ligase can have significantly different activity, and it is essential to adjust the quantity of ligase accordingly, based on the yields of test reactions.

- Different junctions ligate differently. Changing ligase concentration, oligonucleotides concentration, ATP concentration, or pH may help. We have found that for some junctions addition of 30% glycerol dramatically improves the yield.
- T4 DNA ligase often purifies in its adenylated form. Adjust the concentration of ATP in the ligase buffer to achieve the best ligation efficiency.

3.2. Kinetic assay

The phosphorothioate-containing ribozymes can be used to test for a contact with a metal ion, as described in Section 2.2. To extract the affinity of Cd^{2+} for the modified ribozyme and compare it to that for the wt ribozyme (see Scheme 15.1), we measure the observed rate constant for the reaction in Eq. (15.1) as a function of Cd^{2+} concentration. Typically 6–12 Cd^{2+}concentrations are used. For each ribozyme, reactions of the unmodified and sulfur- or amino-containing substrates are followed side-by-side at each Cd^{2+} concentration. All experiments are performed under single-turnover conditions, with ribozyme in excess of the oligonucleotide substrate S, which is added in trace as a radioactive species.

The following protocol is an example for reactions of the *Tetrahymena* group I ribozyme. Change accordingly to your system.

(a) Before starting the protocol, it is essential to carefully plan the timing of the kinetic assays. Prepare enough tubes containing stop solution (50 m*M* EDTA, 90% formamide, 0.01% bromophenol blue, 0.01% xylene cyanol) before starting the experiment. Plan to take at least 5–6 time points for each reaction.

(b) Prefold the wild type and modified ribozymes in 10 m*M* Mg^{2+}, 50 m*M* NaMOPS, pH 7.0, at 50 °C for 30 min. Handling is easiest if the solution is at least 20 μl.

(c) Allow the ribozyme solutions to cool to room temperature for 5 min.

(d) Add the appropriate quantity of the ribozyme solution to a mixture containing the rest of the reagents (*except the radiolabeled oligonucleotide substrate S*), including different amounts of Cd^{2+}, for a final volume of 8–18 μl.

(e) Allow the solutions to equilibrate at 30 °C, or at the temperature the reactions are carried out.

(f) Start the reactions by adding 2 μl of radiolabeled oligonucleotide substrate (S) to the solutions.

(g) Monitor reactions by withdrawing 1.5–2.0 μl of each reaction at different times, and quench them by addition to 4 μl of stop solution (50 m*M* EDTA, 90% formamide, 0.01% bromophenol blu, 0.01% xylene cyanol). Prepare enough tube containing stop solution. The quenched solutions are stable at room temperature, and can be stored until the

last time point is taken. Reactions should be followed for ~3-half lives whenever possible.

(h) Load each quenched reactions, each representing a time point, on denaturing gels containing 20% acrylamide/1× TBE to separate substrates and products by gel electrophoresis. Run reactions of modified and unmodified ribozymes one next to the other to ensure that the products are the same for the two ribozymes, at least as determined from gel mobility. Use bromophenol blue and xylene cyanol as references to determine for how long the gel should run. Important! In case of free substrates with free thiols, all the unreacted acrylamide must be destroyed prior to loading the sample. This is achieved by pouring the gels at least 10 h in advance, and including 5 m*M* DTT in the gel mix. In this case, remember to add the same concentration of DTT to the running buffer.

(i) Dry gels under vacuum, 80 °C, for 1 h.

(j) Place dried gels in a phosphorimager cassette for an appropriate time (do not saturate the signal).

(k) Scan the screen with a phosphorimager to detect the substrate (S) and product (P) bands. Ideally, there should be only two spots per reaction, corresponding to these two species.

(l) Quantify the intensities of the bands corresponding to S and P by using dedicated software.

(m) For each reaction, the pseudo-first-order rate constant for substrate disappearance (k_{obs}) is obtained by plotting the fraction of substrate present at each time point as a function of time, and fitting the data to the following equation:

$$\frac{[S]_t}{[S]_t + [P]_t} = a + (1 - a)e^{-k_{obs}t} \tag{15.5}$$

in which $[S]_t$ and $[P]_t$ are the concentrations of S and P present at time t, and a is the fraction of substrate present at infinite time. For slow reactions, estimate a on the basis of the reaction going to completion. This value should be close to zero.

(n) Values of k_{rel} are determined for each ribozyme at each Cd^{2+} concentration by dividing the observed rate constant for the sulfur-containing substrate by the rate constant of the oxygen-containing substrate.

(o) k_{rel} for each ribozyme are then plotted as a function of Cd^{2+}, and the results fit to Eq. (15.4) to obtain values of $K_{d,app}^{Cd}$.

ACKNOWLEDGMENTS

We thank the numerous researchers who have contributed to and used these approaches, especially Mildred Cohn and Fritz Eckstein for their pioneering efforts. This research was supported by a grant from the NIH (GM 49243) to D. H.

REFERENCES

Christian, E. L. (2005). Identification and characterization of metal ion binding by thiophilic metal ion rescue. *In* "Handbook of RNA Biochemistry, Vol. 1," (R. K. Hartmann, ed.), Wiley-VCH Verlag GmbH & Co., Weinheim.

Christian, E. L., and Yarus, M. (1993). Metal coordination sites that contribute to structure and catalysis in the group I intron from *Tetrahymena*. *Biochemistry* **32,** 4475–4480.

Christian, E. L., Kaye, N. M., and Harris, M. E. (2002). Evidence for a polynuclear metal ion binding site in the catalytic domain of ribonuclease P RNA. *EMBO J.* **21,** 2253–2262.

Cohn, M., Shih, N., and Nick, J. (1982). Reactivity and metal-dependent stereospecificity of the phosphorothioate analogs of ATP in the arginine kinase reaction. Structure of the metal-nucleoside triphosphate substrate. *J. Biol. Chem.* **257,** 7646–7649.

Eckstein, F. (1983). Phosphorothioate analogs of nucleotides—Tools for the investigation of biochemical processes. *Angew. Chem. Int. Ed.* **22,** 423–439.

Forconi, M., Piccirilli, J. A., and Herschlag, D. (2007). Modulation of individual steps in group I intron catalysis by a peripheral metal ion RNA. **13,** 1656–1667.

Forconi, M., Lee, J., Lee, J. K., Piccirilli, J. A., and Herschlag, D. (2008). Functional identification of ligands for a catalytic metal ion in group I introns. *Biochemistry* **47,** 6883–6894.

Golden, B. L., Kim, H., and Chase, E. (2005). Crystal structure of a phage Twort group I ribozyme–product complex. *Nat. Struct. Biol.* **12,** 82–89.

Gordon, P. M., and Piccirilli, J. A. (2001). Metal ion coordination by the AGC triad in domain 5 contributes to group II intron catalysis. *Nat. Struct. Biol.* **8,** 893–898.

Guo, F., Gooding, A. R., and Cech, T. R. (2005). Structure of the *Tetrahymena* ribozyme: Base triple sandwich and metal ion at the active site. *Mol. Cell* **16,** 351–362.

Harris, M. E., and Pace, N. R. (1995). Identification of phosphates involved in catalysis by the ribozyme RNase P RNA. *RNA* **1,** 210–218.

Herschlag, D., and Cech, T. R. (1990). Catalysis of RNA cleavage by the *Tetrahymena Thermophila* ribozyme. 1. Kinetic description of the reaction of an RNA substrate complementary to the active site. *Biochemistry* **29,** 10159–10171.

Hertel, K. J., Herschlag, D., and Uhlenbeck, O. C. (1996). Specificity of hammerhead ribozyme cleavage. *EMBO J.* **15,** 3751–3757.

Ho, C. K., and Shuman, S. (2002). Bacteriophage T4 RNA ligase 2 (gp24.1) exemplifies a family of RNA ligases found in all phylogenetic domains. *Proc. Natl. Acad. Sci. USA* **99,** 12709–12714.

Hougland, J. L., Kravchuk, A. V., Herschlag, D., and Piccirilli, J. A. (2005). Functional identification of catalytic metal ion binding sites within RNA. *PLoS Biol.* **3,** 1536–1548.

Hougland, J. L., Piccirilli, J. A., Forconi, M., Lee, J., and Herschlag, D. (2006). How the group I intron works: A case study of RNA structure and function. *In* "The RNA World," (R. F. Gesteland, T. R. Cech, and J. F. Atkins, eds.), pp. 133–206. Cold Spring Harbor Laboratory Press, Cold Spring Harbor, New York.

Jansen, J. A., McCarthy, T. J., Soukup, G. A., and Soukup, J. K. (2006). Backbone and nucleobase contacts to glucosamine-6-phosphate in the glmS ribozyme. *Nat. Struct. Biol.* **13,** 517–523.

Kazantsev, A. V., and Pace, N. R. (1998). Identification by modification-interference of purine N-7 and ribose 2′-OH groups critical for catalysis by bacterial ribonuclease P. *RNA* **4,** 937–947.

Liao, X., Anjaneyulu, P. S. R., Curley, J. F., Hsu, M., Boehringer, M., Caruthers, M. H., and Piccirilli, J. A. (2001). The *Tetrahymena* ribozyme cleaves a 5′-methylene phosphonate monoester approximately 10^2-fold faster than a normal phosphate diester: Implications for enzyme catalysis of phosphoryl transfer reactions. *Biochemistry* **40,** 10911–10926.

Lipchock, S. V., and Strobel, S. A. (2008). A relaxed active site after exon ligation by the group I intron. *Proc. Natl. Acad. Sci. USA* **105,** 5699–5704.

Luptak, A., and Doudna, J. A. (2004). Distinct sites of phosphorothioate substitution interfere with folding and splicing of the *Anabaena* group I intron. *Nucleic Acids Res.* **32,** 2272–2280.

Maniatis, T., Jeffrey, A., and van deSande, H. (1975). Chain length determination of small double- and single-stranded DNA molecules by polyacrylamide gel electrophoresis. *Biochemistry* **14,** 3787–3794.

Moore, M. J., and Sharp, P. A. (1992). Site-specific modification of pre-mRNA—The 2′-hydroxyl groups at the splice sites. *Science* **256,** 992–997.

Morl, M., Lizano, E., Willkomm, D. K., and Hartmann, R. K. (2005). Production of RNAs with homogeneous 5′ and 3′ ends. *In* ''Handbook of RNA Biochemistry, Vol 1,'' (R. K. Hartmann, ed.), pp. 22–35. Wiley-VCH Verlag GmbH & Co., Weinheim.

Parr, R. G., and Pearson, R. G. (1983). Absolute hardness—Companion parameter to absolute electronegativity. *J. Am. Chem. Soc.* **105,** 7512–7516.

Pearson, R. G. (1963). Hard and soft acids and bases. *J. Am. Chem. Soc.* **85,** 3533–3539.

Pecoraro, V. L., Hermes, J. D., and Cleland, W. W. (1984). Stability constants of magnesium and cadmium complexes of adenine nucleotides and thionucleotides and rate constants for formation and dissociation of magnesium-ATP and magnesium-ADP. *Biochemistry* **23,** 5262–5271.

Piccirilli, J. A., Vyle, J. S., Cartuhers, M. H., and Cech, T. R. (1993). Metal-ion catalysis in the *Tetrahymena* ribozyme reaction. *Nature* **361,** 85–88.

Platts, J. A., Howard, S. T., and Bracke, B. R. F. (1996). Directionality of hydrogen bonds to sulfur and oxygen. *J. Am. Chem. Soc.* **118,** 2726–2733.

Rajagopal, J., Doudna, J. A., and Szostak, J. W. (1989). Stereochemical course of catalysis by the *Tetrahymena* ribozyme. *Science* **244,** 692–694.

Shan, S., and Herschlag, D. (1999). Probing the role of metal ions in RNA catalysis: Kinetic and thermodynamic characterization of a metal ion interaction with the 2′-moiety of the guanosine nucleophile in the *Tetrahymena* group I ribozyme. *Biochemistry* **38,** 10958–10975.

Shan, S., and Herschlag, D. (2000). An unconventional origin of metal-ion rescue and inhibition in the *Tetrahymena* group I ribozyme reaction. *RNA* **6,** 795–813.

Shan, S., Yoshida, A., Piccirilli, J. A., and Herschlag, D. (1999). Three metal ions at the active site of the *Tetrahymena* group I ribozyme. *Proc. Natl. Acad. Sci. USA* **96,** 12299–12304.

Shan, S., Kravchuk, A. V., Piccirilli, J. A., and Herschlag, D. (2001). Defining the catalytic metal ions interactions in the *Tetrahymena* ribozyme reaction. *Biochemistry* **40,** 5161–5171.

Shannon, R. D. (1976). Revised effective ionic radii and systematic studies of interatomic distances in halides and chalcogenides. *Acta Crystallogr.* **A32,** 751–767.

Sjogren, A. J., Petterson, E., Sjoberg, B. M., and Stromberg, R. (1997). Metal Ion interaction with cosubstrate in self-splicing group I introns. *Nucleic Acids Res.* **25,** 648–653.

Sood, V. D., Beattie, T. L., and Collins, R. A. (1998). Identification of phosphate groups involved in metal binding and tertiary interactions in the core of the *Neurospora* vs ribozyme. *J. Mol. Biol.* **282,** 741–750.

Stahley, M. R., and Strobel, S. A. (2005). Structural evidence for a two-metal-ion mechanism of group I intron splicing. *Science* **309,** 1587–1590.

Strauss-Soukup, J. K., and Strobel, S. A. (2000). A chemical phylogeny of group I introns based upon interference mapping of a bacterial ribozyme. *J. Mol. Biol.* **302,** 339–358.

Sun, L., and Harris, M. E. (2007). Evidence that binding of C5 protein to P RNA enhances ribozyme catalysis by influencing active site metal ion affinity. *RNA* **13,** 1505–1515.

Wang, S., Karbstein, K., Peracchi, A., Beigelman, L., and Herschlag, D. (1999). Identification of the hammerhead ribozyme metal ion binding site responsible for rescue of the deleterious effect of a cleavage site phosphorothioate. *Biochemistry* **38,** 14363–14378.

Weinstein, L. B., Jones, B., Cosstick, R., and Cech, T. R. (1997). A second catalytic metal ion in a group I ribozyme. *Nature* **388,** 805–808.

Yoshida, A., Sun, S. G., and Piccirilli, J. A. (1999). A new metal ion interaction in the *Tetrahymena* ribozyme reaction revealed by double sulfur substitution. *Nat. Struct. Biol.* **6,** 318–321.

Yoshida, A., Shan, S., Herschlag, D., and Piccirilli, J. A. (2000). The role of the cleavage site 2′-hydroxyl in the *Tetrahymena* group I ribozyme reaction. *Chem. Biol.* **7,** 85–96.

Zaug, A. J., Grosshans, C. A., and Cech, T. R. (1988). Sequence-specific endoribonuclease activity of the *Tetrahymena* ribozyme—Enhanced cleavage of certain oligonucleotide substrates that form mismatched ribozyme substrate complexes. *Biochemistry* **27,** 8924–8931.

Zhou, P., Tian, F. F., Lv, F. L., and Shang, Z. C. (2009). Geometric characteristics of hydrogen bonds involving sulfur atoms in proteins. *Proteins: Struct. Funct. Bioinformatics* **76,** 151–163.